Nontrivial quantum geometry of degenerate flat bands

Bruno Mera [1] and Johannes Mitscherling [2,3]

[1] *Advanced Institute for Materials Research (WPI-AIMR), Tohoku University, Sendai 980-8577, Japan*
[2] *Max Planck Institute for Solid State Research, Heisenbergstrasse 1, 70569 Stuttgart, Germany*
[3] *Department of Physics, University of California, Berkeley, California 94720, USA*

(Received 16 May 2022; revised 4 August 2022; accepted 17 October 2022; published 31 October 2022)

The importance of the quantum metric in flat-band systems has been noticed recently in many contexts such as the superfluid stiffness, the dc electrical conductivity, and ideal Chern insulators. Both the quantum metric of degenerate and nondegenerate bands can be naturally described via the geometry of different Grassmannian manifolds, specific to the band degeneracies. Contrary to the (Abelian) Berry curvature, the quantum metric of a degenerate band resulting from the collapse of a collection of bands is not simply the sum of the individual quantum metrics. We provide a physical interpretation of this phenomenon in terms of transition dipole matrix elements between two bands. By considering a toy model, we show that the quantum metric gets enhanced, reduced, or remains unaffected depending on which bands collapse. The dc longitudinal conductivity and the superfluid stiffness are known to be proportional to the quantum metric for flat-band systems, which makes them suitable candidates for the observation of this phenomenon.

DOI: 10.1103/PhysRevB.106.165133

Introduction. The quantum metric provides a measure of distance between wave functions in the study of phase transitions [1–3] and is crucial in the modern theory of polarization [4] due to its relation to the size of maximally localized Wannier functions [5,6]. Recently, nontrivial relations between the quantum metric and the Berry curvature have been understood via the underlying Kähler geometry of the space of quantum states [7–9] and have been successfully applied to ideal Chern bands and fractional Chern insulators [10–15]. In materials with highly quenched bandwidth, the quantum metric yields the dominant contribution to the superfluid stiffness [16–26] and the dc electrical conductivity [27]. Here, inequalities for the quantum metric related to the Chern number [7,8,11,28], the Euler characteristic [29], or obstructed Wannier functions [30] result in lower bounds with direct implications for moiré materials such as twisted bilayer graphene [29,31,32] and untwisted heterostructures with flat bands such as rhombohedral trilayer graphene [27]. Especially in the last years, connecting the newly identified importance of the quantum metric in many fields with new insights on fundamental properties of the quantum metric has been established as a powerful research direction [33–66].

Geometric quantities such as the quantum metric arise naturally in the description of interband effects in multiband systems. Interband transitions are described by the product of two Berry connection coefficients, defining transition dipole moments. In transport, such transitions can be induced, for instance, by finite frequencies of the external electric fields [67–74] or virtual band excitations [27,75,76]. Similar contributions are also found for nonuniform electric fields [77,78] and in spectroscopy [79–84]. For two-band systems, the symmetric and antisymmetric parts of the transition dipole moment are proportional to the quantum metric and the Berry curvature, respectively. Since every transition between pairs of bands might be weighted differently, for instance, due to different band occupations, such an identification is possible only in special situations for more than two bands [27], which make general multiband systems promising candidates for new quantum geometric phenomena.

In this paper, we analyze the quantum geometry of degenerate bands by using their relation to the geometry of Grassmannians. It has been noticed before by Peotta and Törmä [16] that the quantum metric is not additive upon collapse of a collection of bands. However, the physical implications have not been investigated so far. The recently discovered quantum metric contribution to the dc electrical conductivity [27] provides a simple theory, which yields a physical quantity proportional to the integrated quantum metric for flat bands and captures the crossover between nondegenerate and (effectively) degenerate bands. For a flat-band toy model, we show that the quantum metric gets enhanced, reduced, or remains unaffected, due to the nontrivial quantum metric of the collapsed bands and, as a consequence, the dc longitudinal conductivity, which we calculate following Ref. [27], exhibits the same behavior. Our results are directly applicable to all the physical observables related to the quantum metric, such as the superfluid stiffness.

The Bloch bundle. We give a self-contained review of the differential geometry of band theory (see also the Supplemental Material (SM) [85]), which is the framework we use. The profitable relation between geometry and quantum mechanics has already been used in different contexts [7–9,73,86–93]. Under the assumption of short-range hopping amplitudes, a tight-binding Hamiltonian with N internal degrees of freedom,

$$H = \sum_{\mathbf{k}} \sum_{i,j=1}^{N} \Psi^{\dagger}_{i,\mathbf{k}} H_{ij}(\mathbf{k}) \Psi_{j,\mathbf{k}}, \tag{1}$$

gives rise to an $N \times N$ Hermitian matrix $H(\mathbf{k}) = [H_{ij}(\mathbf{k})]_{1\leqslant i,j \leqslant N}$, which smoothly depends on momentum $\mathbf{k} \in \mathrm{BZ}^d$ over the d-dimensional Brillouin zone BZ^d. Here, $\Psi^{\dagger}_{i,\boldsymbol{k}}$ and $\Psi_{i,\boldsymbol{k}}$ are fermionic creation and annihilation operators at $\boldsymbol{k}$ and internal degree of freedom i, respectively. For fixed $\mathbf{k}$, the Hermitian matrix $H(\mathbf{k})$ acts on the vector spaces of Bloch wave functions denoted by $\mathcal{E}_{\mathbf{k}}$. The collection of all these vector space forms the *Bloch (vector) bundle* $\mathcal{E} \xrightarrow{\pi} \mathrm{BZ}^d$. The bundle $\mathcal{E}$ comes equipped with a connection $\boldsymbol{\nabla}$—known as the *Berry connection*. It is related to the position operator in the Bloch representation by $\boldsymbol{r} = i\boldsymbol{\nabla}$. In the global gauge of $\mathcal{E}$ provided by $\Psi^{\dagger}_{i,\boldsymbol{k}}|0\rangle$, $i = 1, \dots, N$, ∇ is simply the exterior derivative $d = \sum_{j=1}^{d} dk_j \frac{\partial}{\partial k_j}$. Since $d^2 = 0$, this connection is *flat*, i.e., it has no *curvature*, which is consistent with the fact that position operators commute.

The Hermitian matrix $H(\mathbf{k})$ is diagonalized by the unitary matrix $U(\mathbf{k}) = [|u_{1,\mathbf{k}}\rangle, \dots, |u_{N,\mathbf{k}}\rangle]$ involving Bloch wave functions $|u_{m,\mathbf{k}}\rangle$ as columns. Whereas $H(\mathbf{k})$ and its spectrum, i.e., the energy bands $E_m(\mathbf{k})$, are smooth and globally defined, $U(\mathbf{k})$ does not need to be smoothly defined globally. In fact, at each momentum, it is defined up to multiplication on the right by a unitary matrix preserving the diagonal matrix of eigenvalues of $H(\mathbf{k})$. Thus, the Bloch Hamiltonian induces a splitting of the vector space $\mathcal{E}_{\mathbf{k}} \cong \mathbb{C}^N$ into mutually orthogonal vector subspaces with dimensions given by the degeneracies of the eigenvalues at that point $\mathbf{k} \in \mathrm{BZ}^d$. Provided the eigenvalues do not cross, these decompositions glue together and provide a splitting of the Bloch bundle $\mathcal{E}$ into vector subbundles of ranks given by the degeneracies of the bands. If we write the Berry connection $\boldsymbol{\nabla}$ on $\mathcal{E}$ using the local frame field provided by $U(\mathbf{k})$, we find nontrivial local connection coefficients, i.e., a (local) gauge field

$$A(\mathbf{k}) = U(\mathbf{k})^{-1} dU(\mathbf{k}) = [\langle u_{m,\mathbf{k}}|d|u_{n,\mathbf{k}}\rangle]_{1\leqslant m,n\leqslant N}. \tag{2}$$

The quantity A is the pullback of the Maurer-Cartan 1-form of $\mathrm{U}(N)$ under the locally defined map $\mathbf{k} \mapsto U(\mathbf{k})$. The nonvanishing of A does not violate the flatness of the connection on $\mathcal{E}$, since $dA + A \wedge A = 0$.

Insulators. For band insulators, the ground state is obtained by filling the entire bands below the Fermi level E_F. The *Fermi projector* associated with these occupied bands $P_F(\mathbf{k}) = \Theta(E_F - H(\mathbf{k}))$, with Θ the Heaviside step function, provides a splitting of the Bloch bundle as

$$\mathcal{E} = \mathrm{Im}(P_F) \oplus \mathrm{Ker}(P_F) = \mathrm{Im}(P_F) \oplus \mathrm{Im}(Q_F), \tag{3}$$

where $Q_F(\mathbf{k}) = I_N - P_F(\mathbf{k})$ with identity matrix I_N. The *occupied Bloch bundle* $\mathrm{Im}(P_F)$ is the vector subbundle of $\mathcal{E}$ whose fiber at $\mathbf{k}$ is the image $\mathrm{Im}[P_F(\mathbf{k})]$. $\mathrm{Im}(Q_F)$ and $\mathrm{Ker}(P_F)$ are defined similarly. Although $\mathcal{E}$ is a trivial vector bundle, the subbundles $\mathrm{Im}(P_F)$ and $\mathrm{Im}(Q_F)$ are not necessarily trivial, leading to rich topological effects such as the quantum anomalous Hall effect [94,95]. The Fermi projector defines a map $P_F : \mathrm{BZ}^d \to \mathrm{Gr}_{N_{occ}}(\mathbb{C}^N)$, where $\mathrm{Gr}_{N_{occ}}(\mathbb{C}^N) = \mathrm{U}(N)/[\mathrm{U}(N_{occ}) \times \mathrm{U}(N - N_{occ})]$ denotes the *Grassmannian of N_{occ}-dimensional subspaces of* $\mathbb{C}^N$ with N_{occ} being the number of bands below E_F.

Berry curvature and quantum metric. For a smooth orthogonal projector $P : \mathrm{BZ}^d \to \mathrm{Gr}_r(\mathbb{C}^N)$ of some rank r, the Berry connection $\boldsymbol{\nabla}$ on $\mathcal{E}$ does not necessarily preserve the sections of $\mathrm{Im}(P)$ because the components of Eq. (2), for $|u_{n,\boldsymbol{k}}\rangle$ taking values in $\mathrm{Im}(P)$ and $|u_{m,\boldsymbol{k}}\rangle$ in $\mathrm{Im}(Q)$, can be nontrivial. The composition $P\boldsymbol{\nabla}$, acting on sections of $\mathrm{Im}(P) \subset \mathcal{E}$, defines the projected Berry connection which, in general, is no longer flat. Its curvature, known as the *Berry curvature*, is the 2-form [85]

$$\Omega = (P\boldsymbol{\nabla}) \wedge (P\boldsymbol{\nabla}) = PdP \wedge dPP. \tag{4}$$

The *Abelian Berry curvature* is $F = \mathrm{Tr}(\Omega)$, where the trace is taken over the internal indices.

We obtain further insights and properties by exploring the role of the map P to the relevant Grassmannian. If one recalls the definition of the Fubini-Study Kähler form ω_{FS} on the Grassmannian—a Kähler manifold [96]—one finds that F equals the pullback under P of $2i\omega_{FS}$ [8,9],

$$F = 2iP^*\omega_{FS} = \mathrm{Tr}(PdP \wedge dP). \tag{5}$$

Furthermore, the pullback of the Fubini-Study metric g_{FS} of the Grassmannian defines the *quantum metric*,

$$g = P^* g_{FS} = \mathrm{Tr}(PdPdP) = \tfrac{1}{2}\mathrm{Tr}(dPdP). \tag{6}$$

Using the Cauchy-Schwarz inequality associated with the Hermitian form $g_{FS} + i\omega_{FS}$ of the Grassmannian, it follows that $g^{ii}(\mathbf{k})g^{jj}(\mathbf{k}) - g^{ij}(\mathbf{k})g^{ij}(\mathbf{k}) \geqslant |F^{ij}(\mathbf{k})/2|^2$ for $i, j \in \{1, \dots, d\}$ with $g = \sum_{i,j} g^{ij} dk_i dk_j$ and $F = (1/2)\sum_{i,j} F^{ij} dk_i \wedge dk_j$ [8]. This identity implies an inequality between the Chern number and the quantum volume [7–9,97] and

$$g^{ii}(\mathbf{k}) + g^{jj}(\mathbf{k}) \geqslant |F^{ij}(\mathbf{k})|, \tag{7}$$

which generalizes the result known for two [28] to d dimensions. Equation (7) has been used to identify lower bounds on quantities involving the quantum metric [16,27].

Isolated bands. The previous results can be directly applied to other relevant projectors. When an energy band n is isolated, i.e., it does not cross any other band, there is a well-defined orthogonal projector $P_n(\mathbf{k})$ at each $\mathbf{k} \in \mathrm{BZ}^d$ with fixed rank $N_n \in \{1, \dots, N\}$, which corresponds to the band degeneracy. $P_n(\mathbf{k})$ defines a map $P_n : \mathrm{BZ}^d \to \mathrm{Gr}_{N_n}(\mathbb{C}^N)$. For a *nondegenerate* band $N_n = 1$, P_n assigns the ray associated with the corresponding Bloch wave function $|u_{n,\mathbf{k}}\rangle$ of $H(\mathbf{k})$ to each $\mathbf{k} \in \mathrm{BZ}^d$. We have $\mathrm{Gr}_1(\mathbb{C}^N) \cong \mathbb{C}P^{N-1}$, which is commonly known as *Bloch sphere* for a two-band system. For an N_n-fold degenerate band, the map P_n gives rise to an associated vector bundle $\mathrm{Im}(P_n) \xrightarrow{\pi} \mathrm{BZ}^d$ whose fibers are spanned by an orthonormal basis of corresponding N_n eigenfunctions $|u_{ns,\mathbf{k}}\rangle$, $s = 1, \dots, N_n$. Using Eqs. (6) and (5), the explicit formulas for the quantum metric and the Abelian Berry curvature of band n are [85]

$$g_n(\mathbf{k}) = \sum_{s=1}^{N_n}\sum_{i,j=1}^{d} \langle \partial_i u_{ns,\mathbf{k}}|Q_n(\mathbf{k})|\partial_j u_{ns,\mathbf{k}}\rangle dk_i dk_j, \tag{8}$$

$$F_n(\mathbf{k}) = \sum_{s=1}^{N_n}\sum_{i,j=1}^{d} \langle \partial_i u_{ns,\mathbf{k}}|Q_n(\mathbf{k})|\partial_j u_{ns,\mathbf{k}}\rangle dk_i \wedge dk_j, \tag{9}$$

where $Q_n(\mathbf{k}) = I_N - P_n(\mathbf{k})$ and $\partial_i \equiv \partial/\partial k_i$, $i = 1, \dots, d$.

Nonadditivity of the quantum metric. Let us consider a *split* band projector, i.e., an orthogonal projector P_n of rank N_n which decomposes into the sum of mutually orthogonal projectors

$$P_n(\boldsymbol{k}) = P_1(\boldsymbol{k}) + P_2(\boldsymbol{k}), \tag{10}$$

with P_1 and P_2 having ranks N_1 and N_2, respectively. This situation occurs when two bands described by P_1 and P_2 (effectively) degenerate into one by tuning some external parameter. The main result that we want to emphasize, previously noted in [16], is that the quantum metric g_n of a split band is not generally the sum of the quantum metrics g_1, g_2 of each of the individual bands. Instead,

$$g_n = g_1 + g_2 + \mathrm{Tr}(dP_1 dP_2). \tag{11}$$

This additional term can even render $g_n = 0$ if $P_1 + P_2$ is a constant projector, i.e., if $\mathrm{Im}(P_n)$ is a trivial bundle [85]. In contrast, the Abelian Berry curvature F_n of the split band is equal to the sum of the Abelian Berry curvatures of each band. The upper results can be easily generalized to multiply split bands.

We now give a physical interpretation of the nonadditivity property. If we write $P_i(\boldsymbol{k}) = \sum_{m=1}^{N_i} |u_{im,\boldsymbol{k}}\rangle\langle u_{im,\boldsymbol{k}}|$, $i = 1, 2$, then the mixed term $\mathrm{Tr}(dP_1 dP_2)$ can be written as

$$\mathrm{Tr}(dP_1 dP_2) = -2\sum_{s=1}^{N_1}\sum_{l=1}^{N_2} |\langle u_{2l,\boldsymbol{k}}|d|u_{1s,\boldsymbol{k}}\rangle|^2, \tag{12}$$

which is the sum of the squares of all possible transition dipole matrix elements $i\langle u_{2l,\boldsymbol{k}}|\partial_j|u_{1s,\boldsymbol{k}}\rangle$, $s = 1, \dots, N_1$, $l = 1, \dots, N_2$, $j = 1, \dots, d$, between the two bands. The nonvanishing of this contribution tells us that, if $P_1(\boldsymbol{k})$ and $P_2(\boldsymbol{k})$ described isolated degenerate bands separated by some gap, then states can be excited from one band to another induced, for instance, by finite frequencies of the external electric fields or virtual band excitations.

DC electrical conductivity. We apply the general results presented above to the dc electrical conductivity tensor σ^{ij}, which relates the current and the external electric field via $\mathcal{J}^i = \sum_{j=1}^{d} \sigma^{ij} E^j$. The conductivity tensor can be conveniently decomposed into $\sigma^{ij} = \sigma^{ij}_{\text{intra}} + \sigma^{ij,s}_{\text{inter}} + \sigma^{ij,a}_{\text{inter}}$ [75]. In the following, we focus on the (symmetric) quantum metric contribution [27,75],

$$\sigma^{ij,s}_{\text{inter}} = \frac{e^2}{\hbar}\int \frac{d^d\mathbf{k}}{(2\pi)^d} \sum_{\substack{n,m=1\\ n\neq m}}^{N} w^{\text{inter},s}_{nm}(\mathbf{k})\, g^{ij}_{nm}(\mathbf{k}), \tag{13}$$

with electric charge e, reduced Planck's constant $\hbar$, and summation over pairs of the N bands. We have $g^{ij}_{nm}(\mathbf{k}) \equiv \mathrm{Re}\,[r^i_{nm}(\mathbf{k})\, r^j_{mn}(\mathbf{k})]$ involving the transition dipole matrix element $r^i_{nm} \equiv i\langle u_{n,\mathbf{k}}|\partial_i|u_{m,\mathbf{k}}\rangle$ [cf. Eq. (2)]. Each transition is weighted by $w^{\text{inter},s}_{nm}(\mathbf{k}) \equiv -\pi(E_{n,\mathbf{k}} - E_{m,\mathbf{k}})^2 \int d\epsilon\, f'(\epsilon)\mathcal{A}_n(\mathbf{k},\epsilon)\mathcal{A}_m(\mathbf{k},\epsilon)$, where $\mathcal{A}_n(\mathbf{k},\epsilon) = \Gamma/\{\pi[\Gamma^2 + (\epsilon + \mu - E_{n,\mathbf{k}})^2]\}^{-1}$ is the spectral function of band n with chemical potential μ and phenomenological relaxation rate Γ. $f(\epsilon) = [\exp(\epsilon/k_B T) + 1]^{-1}$ is the Fermi function with Boltzmann constant k_B and temperature T. We present the analogous results for the intraband and the (antisymmetric) Berry curvature contribution $\sigma^{ij}_{\text{intra}}$ and $\sigma^{ij,a}_{\text{inter}}$ in the SM [85].

Conductivity of degenerate bands. We consider r isolated bands. Each band n is N_n-fold degenerate with $E_{n,\mathbf{k}} \equiv E_{(ns),\mathbf{k}}$, where $s = 1, \dots, N_n$. We notice that $w^{\text{inter},s}_{nm} \equiv w^{\text{inter},s}_{(ns)(ml)}$ only depends on the degenerate eigenvalues and are, thus, equal for all $s = 1, \dots, N_n$ and $l = 1, \dots, N_m$. In particular, interband transitions within a degenerate band vanish. Using this, we equivalently write the formula in Eq. (13) as

$$\sigma^{ij,s}_{\text{inter}} = \frac{e^2}{\hbar}\int \frac{d^d\mathbf{k}}{(2\pi)^d} \sum_{\substack{n,m=1\\ n\neq m}}^{r} w^{\text{inter},s}_{nm}(\mathbf{k})\, \widehat{g}^{ij}_{nm}(\mathbf{k}), \tag{14}$$

with summation only over pairs of the r different degenerate subspaces and

$$\widehat{g}^{ij}_{nm}(\mathbf{k}) \equiv \sum_{s=1}^{N_n}\sum_{l=1}^{N_m} \mathrm{Re}\,[i\langle u_{ns,\mathbf{k}}|\partial_i u_{ml,\mathbf{k}}\rangle i\langle u_{ml,\mathbf{k}}|\partial_j u_{ns,\mathbf{k}}\rangle], \tag{15}$$

which includes the remaining summation within the two involved degenerate subspaces. We prove that $\widehat{g}^{ij}_{nm}$ is invariant under $\mathrm{U}(N_n) \times \mathrm{U}(N_m)$-gauge transformations [85], which shows the gauge-invariance of the conductivity in Eq. (13) and each term in Eq. (14).

As a first application, we study a system composed of two independent copies of a single system with Bloch Hamiltonian $H(\mathbf{k})$, with N nondegenerate bands. Then, the eigenvalues $E_{n,\mathbf{k}}$ of the Hamiltonian $H'(\mathbf{k}) \equiv H(\mathbf{k}) \oplus H(\mathbf{k})$ are twofold degenerate with eigenvectors $|u_{n1,\mathbf{k}}\rangle = (|u_{n,\mathbf{k}}\rangle, 0)$ and $|u_{n2,\mathbf{k}}\rangle = (0, |u_{n,\mathbf{k}}\rangle)$, where $|u_{n,\mathbf{k}}\rangle$ is the corresponding eigenvector of $H(\mathbf{k})$. From Eq. (15) it follows that $\widehat{g}'^{ij}_{nm} = 2\,\widehat{g}^{ij}_{nm}$, which is the expected trivial enhancement. Whereas the intraband contribution $\sigma^{ij}_{\text{intra}}$ of an N_n-degenerate band n is always enhanced by a factor N_n in relation to the nondegenerate case [85], this is, however, not generally true for the quantum metric contribution in Eq. (14) as we will see in the following.

Underlying Grassmannian geometry. Using Eqs. (8) and (15), the relation between $\widehat{g}^{ij}_{nm}$ involving a specific degenerate band n and the quantum metric components g^{ij}_n induced by the projection $P_n(\mathbf{k}) = \sum_{s=1}^{N_n} |u_{ns,\mathbf{k}}\rangle\langle u_{ns,\mathbf{k}}|$ onto this band is

$$\sum_{\substack{m=1\\ m\neq n}}^{r} \widehat{g}^{ij}_{nm}(\mathbf{k}) = g^{ij}_n(\boldsymbol{k}). \tag{16}$$

This shows the close relation between the gauge-invariant transition dipole moments defined in Eq. (15) involving an N_n-fold degenerate band and the geometry of the corresponding Grassmannian $\mathrm{Gr}_{N_n}(\mathbb{C}^N)$.

The conductivity in Eq. (14) and the identity (16) differ by the transition-dependent weights $w_{nm}^{\text{inter},s}$. These weights drastically simplify for a clean metal and in flat-band systems. In presence of a $(d-1)$-dimensional Fermi surface, we have

$$\sigma_{\text{inter}}^{ij,s} = -\frac{2\Gamma e^2}{\hbar}\sum_{n=1}^{r}\int \frac{d^d\mathbf{k}}{(2\pi)^d}\, f'(E_{n,\mathbf{k}}-\mu)\, g_n^{ij}(\mathbf{k}), \tag{17}$$

if the band gaps are small on the scale of Γ and the metric is almost constant on the momentum scale, in which the variation of the dispersion is of order Γ [27,75,98]. We see that each band contribution involves the quantum metric that corresponds to the underlying Grassmannian. Since the intraband contribution scales as $1/\Gamma$ in the clean limit, significant corrections due to the quantum metric are expected only for small band gaps $\Delta \sim \Gamma$, for instance, at the onset of order at quantum critical points [98,99]. Let us assume an N_f-fold degenerate flat band f, which is well isolated from all other bands $n \neq f$ with $|E_{n,\mathbf{k}} - E_f| \gg \Gamma$. We set the chemical potential to $\mu = E_f$ and obtain [27]

$$\sigma_{\text{inter}}^{ij,s} = \frac{2}{\pi}\frac{e^2}{\hbar}\int \frac{d^d\mathbf{k}}{(2\pi)^d}\, g_f^{ij}(\mathbf{k}) \equiv \frac{2}{\pi}\frac{e^2}{\hbar}\overline{g}_f^{ij}, \tag{18}$$

where we introduced the quantum metric $\overline{g}_f^{ij}$ of the flat band integrated over the Brillouin zone. The result in Eq. (18) also holds for almost flat bands with $|E_{f,\mathbf{k}} - \mu| \ll \Gamma$. We see that the dominant contribution to the longitudinal conductivity of the flat band is given by the quantum metric of the underlying Grassmannian, since the quasiparticle velocities $\partial_i E_{f,\mathbf{k}} = 0$ (≈ 0) of an (almost) flat band is strongly suppressed [27].

Nontrivial degenerate flat bands. We construct a three-band toy model $H(\mathbf{k})$ with topologically nontrivial flat bands in two dimensions. Let us consider $\vec{n}_\mathbf{k} = \vec{d}_\mathbf{k}/|\vec{d}_\mathbf{k}|$ with $\vec{d}_\mathbf{k} = (\sin k_x, \cos k_y, 1-\cos k_x - \cos k_y)$. We use a spin-1 irreducible representation of SU(2),

$$S_1 = \frac{1}{\sqrt{2}}\begin{bmatrix}0&1&0\\1&0&1\\0&1&0\end{bmatrix},\; S_2 = \frac{1}{\sqrt{2}}\begin{bmatrix}0&i&0\\-i&0&i\\0&-i&0\end{bmatrix},$$
$$S_3 = \begin{bmatrix}-1&0&0\\0&0&0\\0&0&1\end{bmatrix}, \tag{19}$$

in order to define the projectors

$$P_0(\mathbf{k}) = 1 - h_\mathbf{k}^2,\; P_\pm(\mathbf{k}) = \tfrac{1}{2}\left[\pm h_\mathbf{k} + h_\mathbf{k}^2\right], \tag{20}$$

where $h_\mathbf{k} = \vec{n}_\mathbf{k}\cdot\vec{S}$ with $\vec{S} = (S_1, S_2, S_3)$. These projectors correspond to the three momentum-independent eigenvalues 0 and ± 1 of $h_\mathbf{k}$ [85]. We will use the three band energies ε_n in

$$H(\mathbf{k}) = \sum_{n=-,0,+} \varepsilon_n P_n(\mathbf{k}) \tag{21}$$

to discuss the impact of degeneracy on the longitudinal conductivity of flat bands. We have $\sigma_{\text{intra}}^{xx} = 0$ and calculate the longitudinal conductivity $\sigma^{xx} = \sigma_{\text{inter}}^{xx,s}$ via Eq. (13) at zero temperature.

In Fig. 1, we show σ^{xx} as a function of the energy level ε_- for different Γ. We fix the chemical potential μ to the flat-band energies $\varepsilon_0 = -0.5$ (a) and $\varepsilon_+ = 0.5$ (b). In Fig. 1(a), we find a drop of σ^{xx} when $\varepsilon_- = \varepsilon_0$. In contrast, we find a peak when $\varepsilon_- = \varepsilon_+$ in Fig. 1(b). Via Eq. (18), we can relate this behavior to the different quantum metrics of nondegenerate and degenerate bands [85]. If $|\varepsilon_{0/+} - \varepsilon_-| \gg \Gamma$, the flat band at energy $\varepsilon_{0/+}$ is isolated and nondegenerate. We have (a) $\sigma^{xx} = 4\,\overline{g}_0^{xx} = 4\,c$ and (b) $\sigma^{xx} = 4\,\overline{g}_+^{xx} = 2\,c$ in units e^2/h, where $c = \int \frac{d^2\mathbf{k}}{(2\pi)^2}\partial_x\vec{n}_\mathbf{k}\cdot\partial_x\vec{n}_\mathbf{k} \approx 0.454$. If $|\varepsilon_{0/+} - \varepsilon_-| \ll \Gamma$, the flat band is isolated and twofold degenerate. We have (a) $\sigma^{xx} = 4\,\overline{g}_{(-0)}^{xx} = 2\,c$ and (b) $\sigma^{xx} = 4\,\overline{g}_{(+-)}^{xx} = 4\,c$.

In Fig. 2, we show σ^{xx} as a function of the relevant energy scale Γ. We fix $\mu = 1$ to the highest band 1. The band gap to the middle band 2 and lowest band 3 are $\Delta_{12} = 0.1$ and $\Delta_{13} = 10$, respectively. Using Eq. (18), we can relate the obtained conductivity plateaus to the integrated quantum metric, i.e., $\sigma^{xx} = 4\,\overline{g}_1^{xx}$ for $\Gamma \lesssim \Delta_{12}$ and $\sigma^{xx} = 4\,\overline{g}_{(12)}^{xx}$ for $\Delta_{12} \lesssim \Gamma \lesssim \Delta_{13}$ in units e^2/h. Here, we have an effective twofold degeneracy of bands 1 and 2 set by the scale $\Gamma > \Delta_{12}$. In agreement with Fig. 1, we recover the drop and rise of the conductivity in Figs. 2(a) and 2(b), respectively. We have $\overline{g}_+^{xx} = \overline{g}_{(+0)}^{xx} = c/2$ [85], so that the conductivity does not change between the

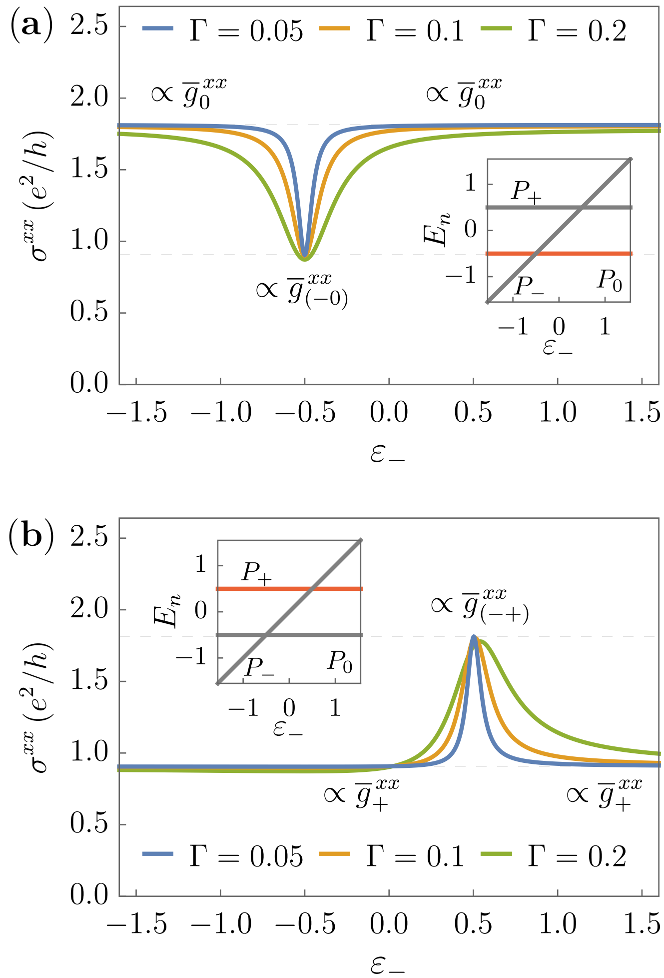

FIG. 1. The longitudinal conductivity σ^{xx} of a flat band is proportional to the corresponding integrated quantum metric $\overline{g}_f^{xx}$ (dashed lines). When the bands become degenerate, we find a pronounced drop for $\mu = \varepsilon_0$ (a) and peak for $\mu = \varepsilon_+$ (b). In the inset, we show the energy levels of the three bands.

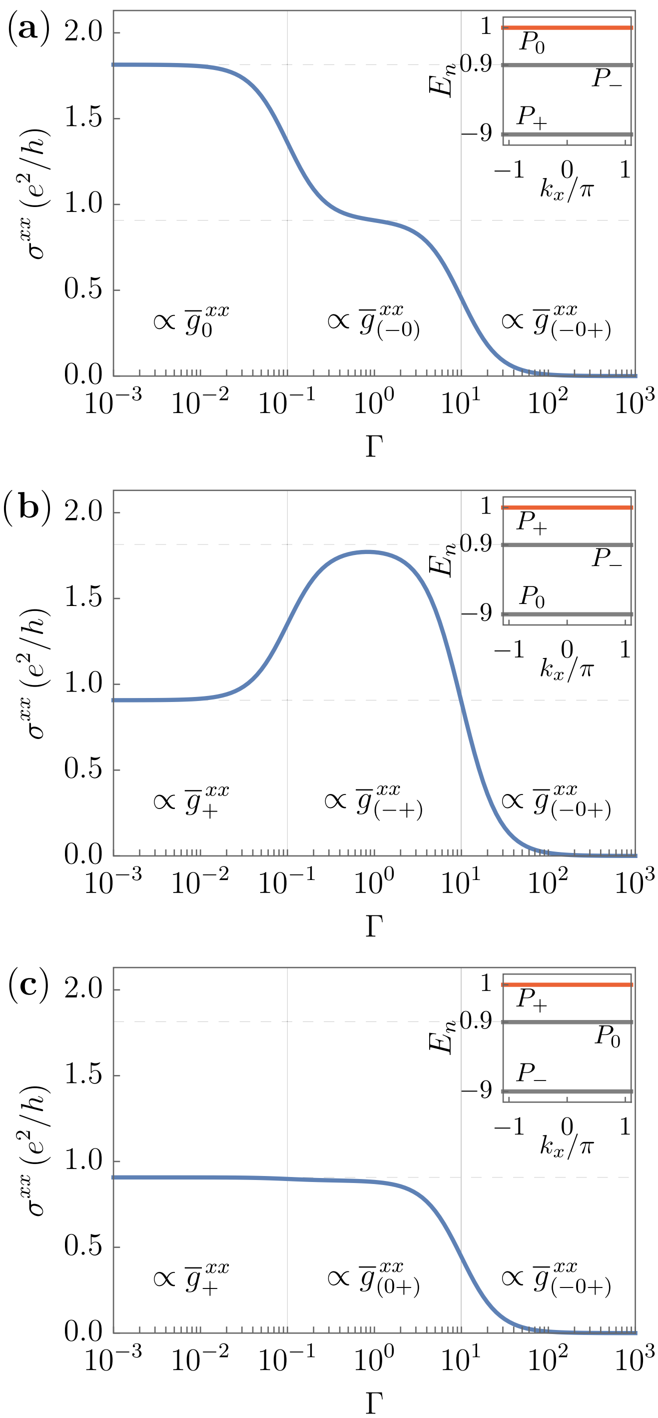

FIG. 2. The longitudinal conductivity σ^{xx} as a function of a phenomenological band broadening Γ for different relative position of the three bands. We understand the value of the observed plateaus (dashed lines) by the quantum metric of the involved one, two, or three bands (inset). The crossovers are given by the band gaps (vertical lines).

nondegenerate and degenerate band in Fig. 2(c). We discuss the crossover behaviors in the SM [85].

Superfluid stiffness. The step from Eq. (13) to Eq. (14) and the application of identity (16) can be analogously used for the superfluid stiffness tensor D_f^{ij} of a degenerate flat band f [16,18,100], where we find

$$D_f^{ij} = \frac{4e^2 U \nu(1-\nu)}{\hbar^2} \int \frac{d^d\boldsymbol{k}}{(2\pi)^d} g_f^{ij}(\boldsymbol{k}), \tag{22}$$

with coupling strength U and filling factor of the band ν. Here, the relevant reference scale for the flat-band degeneracy is U instead of the phenomenological relaxation rate Γ. Thus, we can directly apply Eqs. (7) and (11). Inequalities of the form given in Eq. (7) were used to derive lower bounds for the superfluid stiffness [16]. The nonadditivity property of the quantum metric will manifest itself in the nonadditivity, under (effective) band collapse, of the superfluid stiffness D_f^{ij}. Our result is consistent with previous work where the importance of band degeneracy for the superfluid stiffness was noticed before [16]. It is crucial for twisted bilayer graphene [29].

We note that it has been shown recently that the so-called minimal quantum metric, the metric with minimal trace, should be considered when computing of the superfluid stiffness D_f^{ij} [23].

Conclusions. We have shown how the nonadditivity of the quantum metric upon collapse of a collection of bands manifests itself in physical observables (such as the dc electrical conductivity and the superfluid stiffness). We have given a physical interpretation for the term responsible for failure of additivity in terms of transition dipole matrix elements between two bands. We suggest that this distinguished property may be used to infer quantum metric effects. Furthermore, it provides a new purely quantum-geometrical mechanism for manipulating measurable quantities by changing the underlying degeneracy. It would be interesting to study the effect of nonadditivity of the quantum metric in disordered systems and in systems with interactions. Several direct measurements of the quantum metric have been reported recently [101–108], which might serve as a good starting point for an experimental verification of this effect.

Acknowledgments. We thank M. M. Hirschmann, T. Ozawa, and J. E. Moore for carefully reading through this manuscript and for stimulating comments. B.M. acknowledges very important discussions with T. Ozawa before the starting date of this work, where the peculiar differences between degenerate and nondegenerate band quantum metrics were pointed out. B.M. also acknowledges fruitful discussions with N. Goldman. J.M. thanks J. Ahn, P. M. Bonetti, W. Chen, T. Holder, A. Lau, A. Leonhardt, W. Metzner, and A. Schnyder for stimulating discussions on the role of the quantum metric. We thank K.-E. Huhtinen for valuable discussions. J.M. acknowledges support by the German National Academy of Sciences Leopoldina through Grant No. LPDS 2022-06.

B.M. and J.M. contributed equally to this work.

[1] P. Zanardi and N. Paunković, Ground state overlap and quantum phase transitions, Phys. Rev. E **74**, 031123 (2006).
[2] A. T. Rezakhani, D. F. Abasto, D. A. Lidar, and P. Zanardi, Intrinsic geometry of quantum adiabatic evolution and quantum phase transitions, Phys. Rev. A **82**, 012321 (2010).
[3] A. Carollo, D. Valenti, and B. Spagnolo, Geometry of quantum phase transitions, Phys. Rep. **838**, 1 (2020).
[4] R. Resta, The insulating state of matter: A geometrical theory, Eur. Phys. J. B **79**, 121 (2011).
[5] N. Marzari and D. Vanderbilt, Maximally localized generalized Wannier functions for composite energy bands, Phys. Rev. B **56**, 12847 (1997).
[6] N. Marzari, A. A. Mostofi, J. R. Yates, I. Souza, and D. Vanderbilt, Maximally localized Wannier functions: Theory and applications, Rev. Mod. Phys. **84**, 1419 (2012).
[7] T. Ozawa and B. Mera, Relations between topology and the quantum metric for Chern insulators, Phys. Rev. B **104**, 045103 (2021).
[8] B. Mera and T. Ozawa, Kähler geometry and Chern insulators: Relations between topology and the quantum metric, Phys. Rev. B **104**, 045104 (2021).
[9] B. Mera and T. Ozawa, Engineering geometrically flat Chern bands with Fubini-Study Kähler structure, Phys. Rev. B **104**, 115160 (2021).
[10] D. Varjas, A. Abouelkomsan, K. Yang, and E. J. Bergholtz, Topological lattice models with constant Berry curvature, SciPost Phys. **12**, 118 (2022).
[11] J. Wang, J. Cano, A. J. Millis, Z. Liu, and B. Yang, Exact Landau Level Description of Geometry and Interaction in a Flatband, Phys. Rev. Lett. **127**, 246403 (2021).
[12] J. Wang and Z. Liu, Hierarchy of Ideal Flatbands in Chiral Twisted Multilayer Graphene Models, Phys. Rev. Lett. **128**, 176403 (2022).
[13] P. J. Ledwith, A. Vishwanath, and E. Khalaf, Family of Ideal Chern Flatbands with Arbitrary Chern Number in Chiral Twisted Graphene Multilayers, Phys. Rev. Lett. **128**, 176404 (2022).
[14] C. Northe, G. Palumbo, J. Sturm, C. Tutschku, and E. M. Hankiewicz, Interplay of band geometry and topology in ideal Chern insulators in presence of external electromagnetic fields, Phys. Rev. B **105**, 155410 (2022).
[15] D. Parker, P. Ledwith, E. Khalaf, T. Soejima, J. Hauschild, Y. Xie, A. Pierce, M. P. Zaletel, A. Yacoby, and A. Vishwanath, Field-tuned and zero-field fractional Chern insulators in magic angle graphene, arXiv:2112.13837.
[16] S. Peotta and P. Törmä, Superfluidity in topologically nontrivial flat bands, Nat. Commun. **6**, 8944 (2015).
[17] J. S. Hofmann, E. Berg, and D. Chowdhury, Superconductivity, pseudogap, and phase separation in topological flat bands, Phys. Rev. B **102**, 201112(R) (2020).
[18] P. Törmä, S. Peotta, and B. A. Bernevig, Superconductivity, superfluidity and quantum geometry in twisted multilayer systems, Nat. Rev. Phys. **4**, 528 (2022).
[19] T. Kitamura, T. Yamashita, J. Ishizuka, A. Daido, and Y. Yanase, Superconductivity in monolayer FeSe enhanced by quantum geometry, Phys. Rev. Res. **4**, 023232 (2022).
[20] E. Rossi, Quantum metric and correlated states in two-dimensional systems, Curr. Opin. Solid State Mater. Sci. **25**, 100952 (2021).
[21] N. Verma, T. Hazra, and M. Randeria, Optical spectral weight, phase stiffness, and T_c bounds for trivial and topological flat band superconductors, Proc. Natl. Acad. Sci. USA **118**, e2106744118 (2021).
[22] C. Lewandowski, S. Nadj-Perge, and D. Chowdhury, Does filling-dependent band renormalization aid pairing in twisted bilayer graphene? npj Quantum Mater. **6**, 82 (2021).
[23] K.-E. Huhtinen, J. Herzog-Arbeitman, A. Chew, B. A. Bernevig, and P. Törmä, Revisiting flat band superconductivity: Dependence on minimal quantum metric and band touchings, Phys. Rev. B **106**, 014518 (2022).
[24] A. Lau, S. Peotta, D. I. Pikulin, E. Rossi, and T. Hyart, Universal suppression of superfluid weight by non-magnetic disorder in s-wave superconductors independent of quantum geometry and band dispersion, SciPost Phys. **13**, 086 (2022).
[25] J. S. Hofmann, E. Berg, and D. Chowdhury, Superconductivity, charge density wave, and supersolidity in flat bands with tunable quantum metric, arXiv:2204.02994.
[26] G. Bouzerar, Giant boost of the quantum metric in disordered one-dimensional flat-band systems, Phys. Rev. B **106**, 125125 (2022).
[27] J. Mitscherling and T. Holder, Bound on resistivity in flat-band materials due to the quantum metric, Phys. Rev. B **105**, 085154 (2022).
[28] R. Roy, Band geometry of fractional topological insulators, Phys. Rev. B **90**, 165139 (2014).
[29] F. Xie, Z. Song, B. Lian, and B. A. Bernevig, Topology-Bounded Superfluid Weight in Twisted Bilayer Graphene, Phys. Rev. Lett. **124**, 167002 (2020).
[30] J. Herzog-Arbeitman, V. Peri, F. Schindler, S. D. Huber, and B. A. Bernevig, Superfluid Weight Bounds from Symmetry and Quantum Geometry in Flat Bands, Phys. Rev. Lett. **128**, 087002 (2022).
[31] X. Hu, T. Hyart, D. I. Pikulin, and E. Rossi, Geometric and Conventional Contribution to the Superfluid Weight in Twisted Bilayer Graphene, Phys. Rev. Lett. **123**, 237002 (2019).
[32] A. Julku, T. J. Peltonen, L. Liang, T. T. Heikkilä, and P. Törmä, Superfluid weight and Berezinskii-Kosterlitz-Thouless transition temperature of twisted bilayer graphene, Phys. Rev. B **101**, 060505(R) (2020).
[33] I. Souza and D. Vanderbilt, Dichroic f-sum rule and the orbital magnetization of crystals, Phys. Rev. B **77**, 054438 (2008).
[34] S. Matsuura and S. Ryu, Momentum space metric, nonlocal operator, and topological insulators, Phys. Rev. B **82**, 245113 (2010).
[35] Y.-Q. Ma, S. Chen, H. Fan, and W.-M. Liu, Abelian and non-Abelian quantum geometric tensor, Phys. Rev. B **81**, 245129 (2010).
[36] T. Neupert, C. Chamon, and C. Mudry, Measuring the quantum geometry of Bloch bands with current noise, Phys. Rev. B **87**, 245103 (2013).
[37] M. Kolodrubetz, V. Gritsev, and A. Polkovnikov, Classifying and measuring geometry of a quantum ground state manifold, Phys. Rev. B **88**, 064304 (2013).
[38] Y. Gao, S. A. Yang, and Q. Niu, Field Induced Positional Shift of Bloch Electrons and Its Dynamical Implications, Phys. Rev. Lett. **112**, 166601 (2014).
[39] A. Srivastava and A. Imamoğlu, Signatures of Bloch-Band Geometry on Excitons: Nonhydrogenic Spectra in Transition-Metal Dichalcogenides, Phys. Rev. Lett. **115**, 166802 (2015).

[40] V. V. Albert, B. Bradlyn, M. Fraas, and L. Jiang, Geometry and Response of Lindbladians, Phys. Rev. X **6**, 041031 (2016).
[41] F. Piéchon, A. Raoux, J.-N. Fuchs, and G. Montambaux, Geometric orbital susceptibility: Quantum metric without Berry curvature, Phys. Rev. B **94**, 134423 (2016).
[42] F. Freimuth, S. Blügel, and Y. Mokrousov, Geometrical contributions to the exchange constants: Free electrons with spin-orbit interaction, Phys. Rev. B **95**, 184428 (2017).
[43] M. Kolodrubetz, D. Sels, P. Mehta, and A. Polkovnikov, Geometry and non-adiabatic response in quantum and classical systems, Phys. Rep. **697**, 1 (2017).
[44] M. Iskin, Quantum-metric contribution to the pair mass in spin-orbit-coupled Fermi superfluids, Phys. Rev. A **97**, 033625 (2018).
[45] T. Ozawa and N. Goldman, Extracting the quantum metric tensor through periodic driving, Phys. Rev. B **97**, 201117(R) (2018).
[46] Y. Gao and D. Xiao, Nonreciprocal Directional Dichroism Induced by the Quantum Metric Dipole, Phys. Rev. Lett. **122**, 227402 (2019).
[47] D.-J. Zhang, Q.-h. Wang, and J. Gong, Quantum geometric tensor in $\mathcal{PT}$-symmetric quantum mechanics, Phys. Rev. A **99**, 042104 (2019).
[48] X. Hu, T. Hyart, D. I. Pikulin, and E. Rossi, Quantum-metric-enabled exciton condensate in double twisted bilayer graphene, Phys. Rev. B **105**, L140506 (2022).
[49] Y.-Q. Ma, Euler characteristic number of the energy band and the reason for its non-integer values, arXiv:2001.05946.
[50] D. Rattacaso, P. Vitale, and A. Hamma, Quantum geometric tensor away from equilibrium, J. Phys. Commun. **4**, 055017 (2020).
[51] Y. Zhao, Y. Gao, and D. Xiao, Electric polarization in inhomogeneous crystals, Phys. Rev. B **104**, 144203 (2021).
[52] J. Ahn and N. Nagaosa, Superconductivity-induced spectral weight transfer due to quantum geometry, Phys. Rev. B **104**, L100501 (2021).
[53] P. Bhalla, K. Das, D. Culcer, and A. Agarwal, Quantum geometry induced second harmonic generation, arXiv:2108.04082.
[54] J. Cayssol and J. N. Fuchs, Topological and geometrical aspects of band theory, J. Phys.: Mater. **4**, 034007 (2021).
[55] A. Graf and F. Piéchon, Berry curvature and quantum metric in N-band systems: An eigenprojector approach, Phys. Rev. B **104**, 085114 (2021).
[56] K. Hauser, A. Villegas, and B. Yang, Anomalous Higgs oscillations mediated by Berry curvature and quantum metric, Phys. Rev. B **104**, L180502 (2021).
[57] Y. Hwang, J. Jung, J.-W. Rhim, and B.-J. Yang, Wave-function geometry of band crossing points in two dimensions, Phys. Rev. B **103**, L241102 (2021).
[58] A. Julku, G. M. Bruun, and P. Törmä, Quantum Geometry and Flat Band Bose-Einstein Condensation, Phys. Rev. Lett. **127**, 170404 (2021).
[59] T. Kitamura, J. Ishizuka, A. Daido, and Y. Yanase, Thermodynamic electric quadrupole moments of nematic phases from first-principles calculations, Phys. Rev. B **103**, 245114 (2021).
[60] C. Leblanc, G. Malpuech, and D. D. Solnyshkov, Universal semiclassical equations based on the quantum metric, Phys. Rev. B **104**, 134312 (2021).
[61] A.-G. Penner, F. von Oppen, G. Zaránd, and M. R. Zirnbauer, Hilbert Space Geometry of Random Matrix Eigenstates, Phys. Rev. Lett. **126**, 200604 (2021).
[62] C. Wang, Y. Gao, and D. Xiao, Intrinsic Nonlinear Hall Effect in Antiferromagnetic Tetragonal CuMnAs, Phys. Rev. Lett. **127**, 277201 (2021).
[63] C. Xiao, H. Liu, J. Zhao, S. A. Yang, and Q. Niu, Thermoelectric generation of orbital magnetization in metals, Phys. Rev. B **103**, 045401 (2021).
[64] A. Zhang, Revealing Chern number from quantum metric, Chin. Phys. B **31**, 040201 (2021).
[65] A. Abouelkomsan, K. Yang, and E. J. Bergholtz, Quantum Metric Induced Phases in Moiré Materials, arXiv:2202.10467.
[66] Y.-P. Lin and W.-H. Hsiao, Band geometry from position-momentum duality at topological band crossings, Phys. Rev. B **105**, 075127 (2022).
[67] Y. Gao, Y. Zhang, and D. Xiao, Tunable Layer Circular Photogalvanic Effect in Twisted Bilayers, Phys. Rev. Lett. **124**, 077401 (2020).
[68] T. Holder, D. Kaplan, and B. Yan, Consequences of time-reversal-symmetry breaking in the light-matter interaction: Berry curvature, quantum metric, and diabatic motion, Phys. Rev. Res. **2**, 033100 (2020).
[69] W. Chen and W. Huang, Quantum-geometry-induced intrinsic optical anomaly in multiorbital superconductors, Phys. Rev. Res. **3**, L042018 (2021).
[70] L. Liang, P. O. Sukhachov, and A. V. Balatsky, Axial Magnetoelectric Effect in Dirac Semimetals, Phys. Rev. Lett. **126**, 247202 (2021).
[71] Q. Ma, A. G. Grushin, and K. S. Burch, Topology and geometry under the nonlinear electromagnetic spotlight, Nat. Mater. **20**, 1601 (2021).
[72] H. Watanabe and Y. Yanase, Chiral Photocurrent in Parity-Violating Magnet and Enhanced Response in Topological Antiferromagnet, Phys. Rev. X **11**, 011001 (2021).
[73] J. Ahn, G.-Y. Guo, N. Nagaosa, and A. Vishwanath, Riemannian geometry of resonant optical responses, Nat. Phys. **18**, 290 (2022).
[74] Z. Li, Y. Gao, Y. Gu, S. Zhang, T. Iitaka, and W. M. Liu, Berry curvature induced linear electro-optic effect in chiral topological semimetals, Phys. Rev. B **105**, 125201 (2022).
[75] J. Mitscherling, Longitudinal and anomalous Hall conductivity of a general two-band model, Phys. Rev. B **102**, 165151 (2020).
[76] M. Pickem, E. Maggio, and J. M. Tomczak, Prototypical many-body signatures in transport properties of semiconductors, Phys. Rev. B **105**, 085139 (2022).
[77] M. F. Lapa and T. L. Hughes, Semiclassical wave packet dynamics in nonuniform electric fields, Phys. Rev. B **99**, 121111(R) (2019).
[78] V. Kozii, A. Avdoshkin, S. Zhong, and J. E. Moore, Intrinsic Anomalous Hall Conductivity in a Nonuniform Electric Field, Phys. Rev. Lett. **126**, 156602 (2021).
[79] T. Ozawa and N. Goldman, Probing localization and quantum geometry by spectroscopy, Phys. Rev. Res. **1**, 032019(R) (2019).
[80] R. L. Klees, G. Rastelli, J. C. Cuevas, and W. Belzig, Microwave Spectroscopy Reveals the Quantum Geometric Tensor of Topological Josephson Matter, Phys. Rev. Lett. **124**, 197002 (2020).

[81] R. L. Klees, J. C. Cuevas, W. Belzig, and G. Rastelli, Ground-state quantum geometry in superconductor-quantum dot chains, Phys. Rev. B **103**, 014516 (2021).

[82] G. E. Topp, C. J. Eckhardt, D. M. Kennes, M. A. Sentef, and P. Törmä, Light-matter coupling and quantum geometry in moiré materials, Phys. Rev. B **104**, 064306 (2021).

[83] G. von Gersdorff and W. Chen, Measurement of topological order based on metric-curvature correspondence, Phys. Rev. B **104**, 195133 (2021).

[84] W. Chen and G. von Gersdorff, Linear response theory of Berry curvature and quantum metric in solids, arXiv:2202.03494.

[85] See Supplemental Material at http://link.aps.org/supplemental/10.1103/PhysRevB.106.165133 with further details on (i) the differential geometry of band theory, (ii) the theory for the dc electrical conductivity of degenerate bands, (iii) the discussion on gauge invariance of the relevant quantities in the context of degenerate bands, and (iv) two toy models on the collapse of bands including how the quantum geometry changes according to the degeneracy.

[86] J. P. Provost and G. Vallee, Riemannian structure on manifolds of quantum states, Commun. Math. Phys. **76**, 289 (1980).

[87] F. Wilczek and A. Zee, Appearance of Gauge Structure in Simple Dynamical Systems, Phys. Rev. Lett. **52**, 2111 (1984).

[88] J. Anandan and Y. Aharonov, Geometry of Quantum Evolution, Phys. Rev. Lett. **65**, 1697 (1990).

[89] A. Ashtekar and T. A. Schilling, *Geometrical Formulation of Quantum Mechanics*, edited by A. Harvey, On Einstein's Path: Essays in Honor of Engelbert Schucking (Springer, New York, 1999), pp. 23–65.

[90] J. Alvarez-Jimenez, D. Gonzalez, D. Gutiérrez-Ruiz, and J. D. Vergara, Geometry of the parameter space of a quantum system: Classical point of view, Ann. Phys. **532**, 1900215 (2020).

[91] D. Gonzalez, D. Gutiérrez-Ruiz, and J. David Vergara, Phase space formulation of the Abelian and non-Abelian quantum geometric tensor, J. Phys. A: Math. Theor. **53**, 505305 (2020).

[92] T. Holder, Electrons flow like falling cats: Deformations and emergent gravity in quantum transport, arXiv:2111.07782.

[93] T. B. Smith, L. Pullasseri, and A. Srivastava, Momentum-space gravity from the quantum geometry and entropy of Bloch electrons, Phys. Rev. Res. **4**, 013217 (2022).

[94] D. J. Thouless, M. Kohmoto, M. P. Nightingale, and M. den Nijs, Quantized Hall Conductance in a Two-Dimensional Periodic Potential, Phys. Rev. Lett. **49**, 405 (1982).

[95] Q. Niu, D. J. Thouless, and Y.-S. Wu, Quantized Hall conductance as a topological invariant, Phys. Rev. B **31**, 3372 (1985).

[96] A. C. da Silva, *Lectures on Symplectic Geometry* (Springer, Berlin, Heidelberg, 2008).

[97] B. Mera, A. Zhang, and N. Goldman, Relating the topology of Dirac Hamiltonians to quantum geometry: When the quantum metric dictates Chern numbers and winding numbers, SciPost Phys. **12**, 018 (2022).

[98] J. Mitscherling and W. Metzner, Longitudinal conductivity and Hall coefficient in two-dimensional metals with spiral magnetic order, Phys. Rev. B **98**, 195126 (2018).

[99] P. M. Bonetti, J. Mitscherling, D. Vilardi, and W. Metzner, Charge carrier drop at the onset of pseudogap behavior in the two-dimensional Hubbard model, Phys. Rev. B **101**, 165142 (2020).

[100] L. Liang, T. I. Vanhala, S. Peotta, T. Siro, A. Harju, and P. Törmä, Band geometry, Berry curvature, and superfluid weight, Phys. Rev. B **95**, 024515 (2017).

[101] L. Asteria, D. T. Tran, T. Ozawa, M. Tarnowski, B. S. Rem, N. Fläschner, K. Sengstock, N. Goldman, and C. Weitenberg, Measuring quantized circular dichroism in ultracold topological matter, Nat. Phys. **15**, 449 (2019).

[102] X. Tan, D.-W. Zhang, Z. Yang, J. Chu, Y.-Q. Zhu, D. Li, X. Yang, S. Song, Z. Han, Z. Li, Y. Dong, H.-F. Yu, H. Yan, S.-L. Zhu, and Y. Yu, Experimental Measurement of the Quantum Metric Tensor and Related Topological Phase Transition with a Superconducting Qubit, Phys. Rev. Lett. **122**, 210401 (2019).

[103] A. Gianfrate, O. Bleu, L. Dominici, V. Ardizzone, M. De Giorgi, D. Ballarini, G. Lerario, K. W. West, L. N. Pfeiffer, D. D. Solnyshkov, D. Sanvitto, and G. Malpuech, Measurement of the quantum geometric tensor and of the anomalous Hall drift, Nature (London) **578**, 381 (2020).

[104] M. Yu, P. Yang, M. Gong, Q. Cao, Q. Lu, H. Liu, S. Zhang, M. B. Plenio, F. Jelezko, T. Ozawa, N. Goldman, and J. Cai, Experimental measurement of the quantum geometric tensor using coupled qubits in diamond, Natl. Sci. Rev. **7**, 254 (2020).

[105] X. Tan, D.-W. Zhang, W. Zheng, X. Yang, S. Song, Z. Han, Y. Dong, Z. Wang, D. Lan, H. Yan, S.-L. Zhu, and Y. Yu, Experimental Observation of Tensor Monopoles with a Superconducting Qudit, Phys. Rev. Lett. **126**, 017702 (2021).

[106] H. Tian, S. Che, T. Xu, P. Cheung, K. Watanabe, T. Taniguchi, M. Randeria, F. Zhang, C. N. Lau, and M. W. Bockrath, Evidence for flat band Dirac superconductor originating from quantum geometry, arXiv:2112.13401.

[107] M. Yu, D. Li, J. Wang, Y. Chu, P. Yang, M. Gong, N. Goldman, and J. Cai, Experimental estimation of the quantum Fisher information from randomized measurements, Phys. Rev. Res. **3**, 043122 (2021).

[108] M. Chen, C. Li, G. Palumbo, Y.-Q. Zhu, N. Goldman, and P. Cappellaro, A synthetic monopole source of Kalb-Ramond field in diamond, Science **375**, 1017 (2022).